EXPLORATION OF BASIN STRUCTURE BY MICROTREMOR ARRAY TECHNIQUE FOR ESTIMATION OF LONG-PERIOD GROUND MOTION

Hiroaki YAMANAKA[1], Nobuyuki YAMADA[2], Hiroaki SATO[3], Seiji OIKAWA[4], Yoshihisa OGATA[5], Katsumi KURITA[6], Kazuoh SEO[7] And Yoshihiro KINUGASA[8]

SUMMARY

Long-period microtremor array measurements were conducted at 27 sites in the southern part of the Kanto basin, Japan to know deep S-wave profiles for the purpose of estimation of long-period strong ground motion. Temporary arrays with 7 stations were deployed in circles with radius of 0.2 to 2 km to measure vertical microtremors at each site. Phase velocities at periods from 0.5 to 5 sec were estimated from a frequency-wavenumber spectral analysis of array records. They are dispersive suggesting propagation of Rayleigh waves. Each phase velocity was inverted to a 1D S-wave profile by an inversion method based on a genetic algorithm. A 3- or 4-layers model to a depth of the basement with an S-wave velocity of 3 km/sec was constructed at each site.

INTRODUCTION

Estimation of long-period strong ground motion is one of the important subjects in earthquake engineering for seismic design of large man-made structures. Since the 1985 Mexico earthquake, many studies were devoted to understand long-period strong motion observed at sites in the valley of the Mexico City. Although several numerical studies could simulate elongation of duration due to the long-period ground motion [e.g., Kawase and Aki, 1989], quantitative reconstruction of the observed motion contains still difficult problems. This is mainly due to lack of our knowledge of physical parameters in subsurface structure in the Mexico City. We encountered similar problems in strong motion estimation at most of sites on basins with deep sediments. Recently, three-dimensional numerical simulations of long-period ground motion in large basins were conducted [e.g., Olson et al., 1996; Sato et al., 1999]. The lack of subsurface structural data becomes a more serious problem in prediction of strong ground motion using a three-dimensional numerical technique that requires a 3D model. In this research, we conducted explorations of S-wave velocity profiles in the Kanto sedimentary basin, Japan, by a microtremor array technique. First, we present our methodology to estimate an S-wave profile. They are mainly array analysis of records to determine phase velocity of Rayleigh waves and inversion of the phase velocity by genetic algorithms. Then, results of measurements of long-period microtremors are shown.

METHODS

Microtremor array techniques were actively developed in Japan [Horike, 1996]. It is assumed in the methods that microtremors consist of surface waves propagating from a lot of sources. We, therefore, observe vertical microtremors, which are mainly composed of Rayleigh waves. For example, Horike [1985] observed vertical microtremors in an array, and found a systematic variation of phase velocity with increasing period. This

[1] *Tokyo Institute of Technology, Yokohama, Japan*
[2] *Tokyo Institute of Technology, Yokohama, Japan*
[3] *Central Research Institute of Electric Power Industry, Abiko, Japan*
[4] *Tokyo Institute of Technology, Yokohama, Japan*
[5] *Tokyo Institute of Technology, Yokohama, Japan*
[6] *Tokyo Institute of Technology, Yokohama, Japan*
[7] *Tokyo Institute of Technology, Yokohama, Japan*
[8] *Tokyo Institute of Technology, Yokohama, Japan*

dispersion was interpreted as phase velocity of Rayleigh waves. Therefore, it is possible to deduce subsurface structure by a phase velocity inversion developed in earthquake seismology. In Japan, such microtremor array technique is becoming a popular technique to know an S-wave profile of sedimentary layers [e.g., Horike, 1996].

Figure 1 shows the procedure of data processing in the microtremor array exploration. First we installed vertical seismometers in an array, and measured microtremors simultaneously. Then, a frequency-wavenumber (f-k) spectral analysis was applied to the array data. We used the method by Capon [1969] for analysis of data from an arbitrary array configuration. Once f-k spectra have been obtained, we could estimate phase velocity at each period from a wavenumber for the maximum peak of each f-k spectrum. Repeating these procedures for every f-k spectra, we obtained a phase velocity dispersion curve that corresponds to Rayleigh wave phase velocity.

Next, we invert Rayleigh wave phase velocity obtained from microtremors data to a 1D S-wave velocity profile by an inversion method. Several inversion algorithms have been already developed in seismological community to know crustal and/or mantle structures using linealized least square approaches. In this study, we applied an inversion method based on genetic algorithms by Yamanaka and Ishida [1996]. In the inversion, subsurface structural models are searched by minimizing the misfit that is defined by L1-norm of differences between observed and calculated phase velocities. Theoretical phase velocity is calculated by a matrix method assuming a multi-layered model. Unknown parameters in the inversion are S-wave velocity and thickness for each layer. The other parameters are treated as follows; P-wave velocity is derived using an empirical relation with S-wave velocity, and density is fixed in the inversion. First, 20 models are randomly generated and are processed by genetic operations where models with smaller misfit can survive more in the next generation and worse models are replaced more by newly generated models. One of the advantages of the method is no requirement of a specific initial model that is necessary in linealized least square methods. Since this method is a global optimization method, trapping at local minimum solutions is of less problems than that in least square methods.

MEASUREMENTS

The investigated area is the southern Kanto basin, which is located in the central part of Japan. As can be seen in the basement depth map by Suzuki [1999] in Fig. 2, the Kanto basin is covered with Quaternary and Tertiary sediments having thickness of 4 km at the maximum. In the west of the area, Kanto mountain area, the basement exists near the surface, and it gradually increases its depth toward the center of the basin. Relatively hard sedimentary layers can be seen in the southern end of the area.

We observed microtremors at 27 temporary sites as shown in Fig. 2. The measurements were done in two series. One consists of the measurements in the southwestern part of the basin, where the sites are densely distributed. Another series of the measurements was made in the southeastern part of the basin. It is noted that array measurements of microtremors in similar period ranges were done in the northern part of the basin [e.g., Matsuoka et al., 1996; Sato et al., 1998; Yamanaka et. al, 1994; Yamanaka et al., 1995].

At each site, 2 to 3 arrays with different array sizes were deployed by installing 7 seismometers with station spacing of 0.2 to 3 km. An example of configuration of stations in these arrays is shown in Fig. 3. At each station, we installed an accelerometer or a velocity seismometer, an amplifier, and a digital recorder with a clock signal, which was calibrated with an accuracy of less than 0.01 sec by GPS timing signal. Output signals from the amplifier were digitized every 0.01 sec. Recording was started with a timer and continued for 30 to 90 minutes in one array configuration.

RESULTS

F-k Spectral Analysis

Examples of the f-k spectral analysis for microtremor array data are explained by showing results to estimate phase velocity at NGT. Figure 4 shows vertical ground velocities observed at 7 stations in the small array at the site. We can clearly see long-period components that are coherent with each other. We divided all the records into a dataset with duration of 327.68 seconds. These data were used for the f-k spectral analysis. Examples of the f-k spectra obtained for various periods are shown in Fig. 5. A single peak is found in the f-k spectra at the long-periods, while several peaks are identified in the short-period f-k spectra, suggesting complicated

microtremor wave fields. Frequency-dependent phase velocity and propagation direction were estimated from a wavenumber whose spectral amplitude is the largest. By repeating these processes to all the dataset, we could finally estimate a phase velocity by taking average of all the phase velocities at each period as shown in Fig. 6. The phase velocity shows dispersive features that suggest propagation of Rayleigh waves.

We applied the above processing to the microtremor data at all the sites to obtain phase velocities. The phase velocities estimated at the sites along A-B and A-C lines in Fig. 1 are shown in Fig. 7. The phase velocities at the sites in the western basin edge (HOJ, OSH) are higher than those at the sites in the center of the basin. The phase velocities in the southern end of the basin (ZUS, MSK) are also high, suggesting a reduction of the sediment thickness. However, the phase velocity in the southern end of the Boso Peninsula (TYM) is not so high. This indicates the existence of an up-rift structure of the basement. It is noted that the phase velocities at the sites in the eastern part of the basin are lower than those in the western part at periods of less than 2 sec. This can be interpreted as a systematic difference of geological structure between the two parts of the basin.

Genetic Inversion

The phase velocity estimated at each site is inverted to an S-wave velocity profile by the genetic inversion. In the inversion of all the phase velocities, we assumed a 3- or 4-layers model, because there are 4 major geological formations in the area. They are, namely, Quaternary layer, two Tertiary layers and basement. The search limits of S-wave velocity and thickness are tabulated in Table 1. We conducted 10 inversions with 100 generations using different seeds of random numbers.

Table 1 Search limits in genetic inversion of phase velocity at NGT

No. layer	Vs (km/sec)	H (km)	ρ (ton/m^3)
1	0.2~0.9	0.05~0.80	1.8
2	0.6~1.3	0.30~1.50	2.0
3	1.0~2.0	0.30~2.00	2.3
4	3.0	∞	2.5

We, here, shows results of the inversion of the phase velocity observed at NGT as an example. Figure 8 shows the variation of the misfit with increasing generations. The misfit in the figure is average of results of all 10 inversions. The misfit decreases rapidly in the first 10 generations, and then it almost converges at the 30th generation. As well known, there are local minimum solutions in a phase velocity inversion, because of non-linearity of any misfit function. We, therefore, examined all the investigated models in the genetic inversion using an idea of acceptable solution by Lomax and Snieder (1994). The acceptable solutions are defined as models that have misfits less than a certain value. We can estimate a statistical distribution of the model space using acceptable solutions, like important sampling in Monte Carlo simulation. First, we used the acceptable level that is 1.10 times larger than the minimum misfit of all the models. Figure 9a shows the distribution of the parameters of all the acceptable solutions. The parameters of the first layer are converging at a single point with high resolution. S-wave velocity for the 2nd layer is also resolved well, while its thickness distributes widely. However, the distribution of the parameters for the third layer shows three local concentrations in the model space. This suggests that there are at least three local or global minimums. Then, the acceptable misfit is decreased to be 1.04 of the minimum misfit. The parameter distributions are shown in Fig.9b. All the parameters concentrate at a single point. The parameters of the acceptable solutions in Fig. 9b are averaged to obtain a final model. The determined model is displayed in Fig. 10. The comparison between the observed and theoretical phase velocities is shown in Fig, 6. The theoretical phase velocity well explains the observed one.

The above inversion was applied to all the phase velocities obtained. The inverted models along the A-B and A-C lines are shown in Fig. 11. The profiles along the A-B line show a typical basin shape, which is characterized by a decrease of the sediment thickness in the both ends of the line. It is noted that the S-wave velocity of the top layer in the eastern part of the basin is lower than those at the sites in the western part. The profiles at the northwestern end of the A-C line show the similar basin margin features. However, the sediments do not significantly reduce their thickness in the eastern margin of the basin (TYM).

CONCLUSIONS

In this study, the microtremor array technique was applied to know deep S-wave profiles in the southern part of

the Kanto basin, Japan. The phase velocities of Rayleigh waves were estimated at 27 sites by the frequency wavenumber spectral analysis of array records of vertical microtremors at periods from 0.5 to 5 seconds. Genetic inversion were, then, applied to the phase velocities to deduce S-wave profiles of sedimentary layers down to a depth of the basement with an S-wave velocity of 3 km/sec. This case study clearly indicates that the microtremor array technique is one of the promising exploration methods for a deep S-wave profile in a basin.

We are now trying to simulate long-period earthquake motion in the basin by considering a 3D-basin structure [Yamada and Yamanaka, 2000]. As can be seen in Fig, 1, existing information on the 3D-basin structure is not enough to cover entire region of the basin. Subsurface structural data at some parts are unknown. Because of such uncertainties, reconstruction of observed ground motion by a 3D numerical modeling is still difficult task. We, therefore, continue to conduct microtremor array measurements to fill the information gaps of 3D structure of the basin. Furthermore, we will make array measurements at such a region where observed ground motion can not be well reconstructed by synthetics. These strategic microtremor array measurements can be done with a close cooperation with investigation on numerical 3D simulation of earthquake ground motion.

REFERENCES

Capon, J.(1969), "High resolution frequency wavenumber spectrum analysis", *Proc. IEEE*, **57**, pp1408-1418.

Horike, M. (1985), "Inversion of phase velocity of long-period microtremors to the S-wave velocity structure down to the basement in urbanized areas", *J. Phys. Earth*, **33**, pp59-96.

Horike, M. (1996), "Geophysical exploration using microtremor measurements", *Proc. 11th World Conf. Earthq. Eng.*, Paper No. 2033.

Kawase, H. and Aki, K. (1989), "A study on the response of a soft basin for incident S, P, and Rayleigh waves with special reference to the long duration observed in Mexico City", *Bull. Seis. Soc. Am.*, **79**, pp1361-1382.

Lomax, A. and Snieder, R. (1994), "Finding of acceptable solutions with a genetic algorithm with application of surface wave group velocity dispersion in Europe" ,*Geophy. Res. Lett.*, **21**, pp2617-2620

Matsuoka, T., Umezawa, N., and Makishima, H. (1996), "Experimental studies on the applicability of the spatial autocorrelation method for estimation of geological structures using microtremors", *BUTSURI-TANSA* (Geophysical Exploration), **49**, pp26-41 (in Japanese).

Olson, K.B, and Archuleta, R.J. (1996), "Three-dimensional simulation of earthquakes on the Los Angeles fault system", *Bull. Seis. Soc. Am.*, **86**, pp575-596.

Sato, T, Graves, R.W. and Somerville, P.G. (1999), "Three-dimensional finite-difference simulations of long-period strong motions in the Tokyo Metropolitan area using the 1990 Odawara earthquake (Mj 5.1) and the Great 1923 Kanto earthquake (Ms 8.2) in Japan", *Bull. Seis. Soc. Am.*, **89**, pp579-607

Sato, H., Higashi, S., Sato, K., Kurita, K., Yamanaka, H., Seo, K. (1998), "Exploration of deep S-wave velocity structure for estimation of long-period earthquake ground motion in the northern Kanto plain", *Summaries of Technical papers of Annual Meeting*, Architectural Institute of Japan, **B-2**, pp251-252 (in Japanese)

Suzuki, H. (1999), "Deep geological structure and seismic activity in the Tokyo Metropolitan area", *Journal Geography*, **108**, pp336-339 (in Japanese).

Yamada, N. and Yamanaka, H. (2000), "Three-dimensional finite difference simulation of long-period seismic wave propagation in the Kanto plain, Japan", *submitted to 12WCEE*, New Zealand.

Yamanaka, H. and Ishida, H. (1996), "Application of genetic algorithms to an inversion of surface-wave dispersion data", *Bull. Seis. Soc. Am.*, **86**, pp436-444

Yamanaka, H., Furuya, S., Nozawa, T., Sasaki, T., and Takai, T. (1995), "Array measurements of long-period microtremors in the Kanto plain -Estimation of S-wave velocity structure at Koto", *J. Struct. Constrr. Eng.*, Architectural Institute of Japan, **478**, pp99-105 (In Japanese)

Yamanaka H., Takemura, M., Ishida, H., Ikeura, T., T Nozawa,. Sasaki, T., and M. Niwa (1994), "Array measurements of long-period microtremors and estimation of S-wave velocity structure in the western part of the Tokyo Metropolitan area", *J. Seism. Soc. Japan (Zisin)*, **47**, pp163-172 (in Japanese).

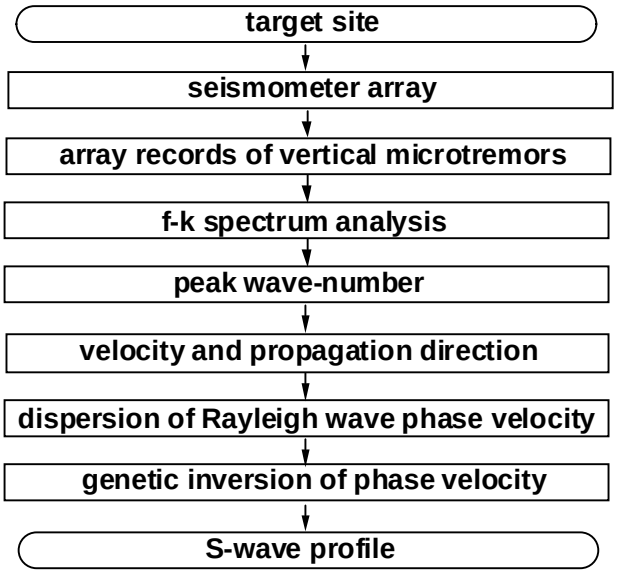

Fig. 1 Flow of data processing in microtremor array technique.

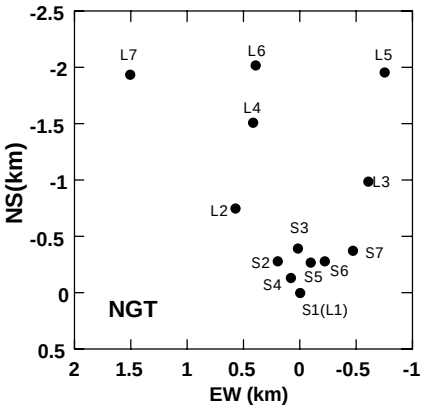

Fig. 3 Array configuration at NGT.

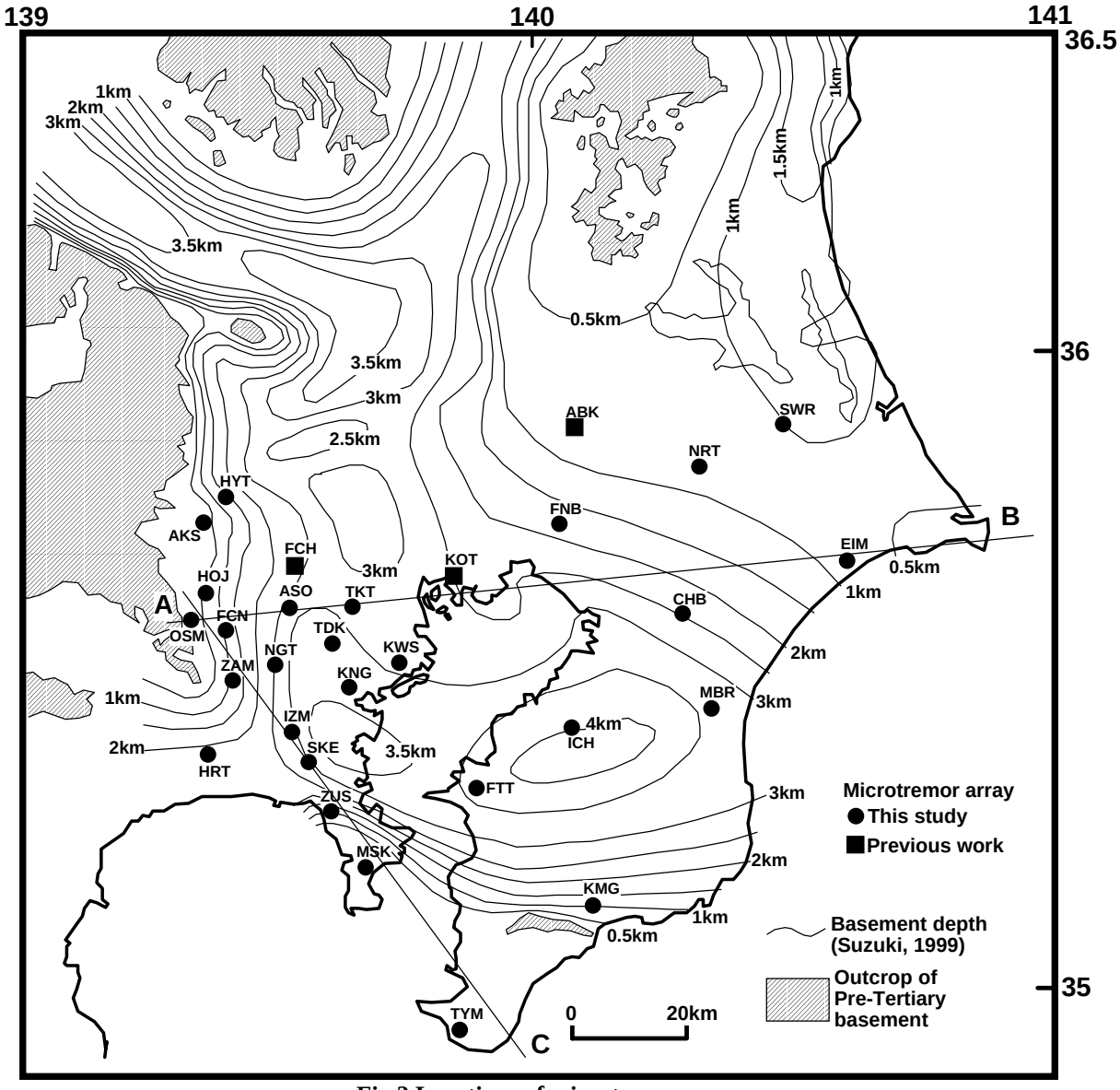

Fig.2 Locations of microtremor arrays.

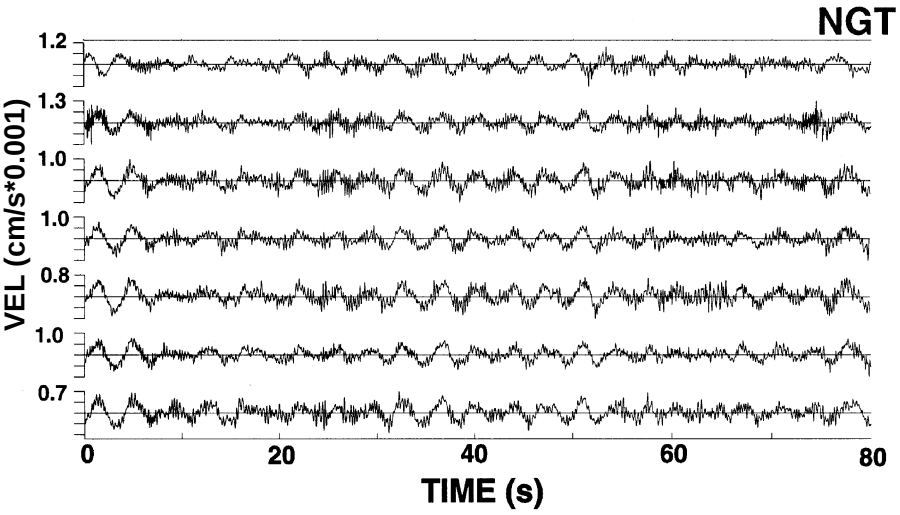

Fig. 4 Example of vertical ground velocities observed in small array at NGT.

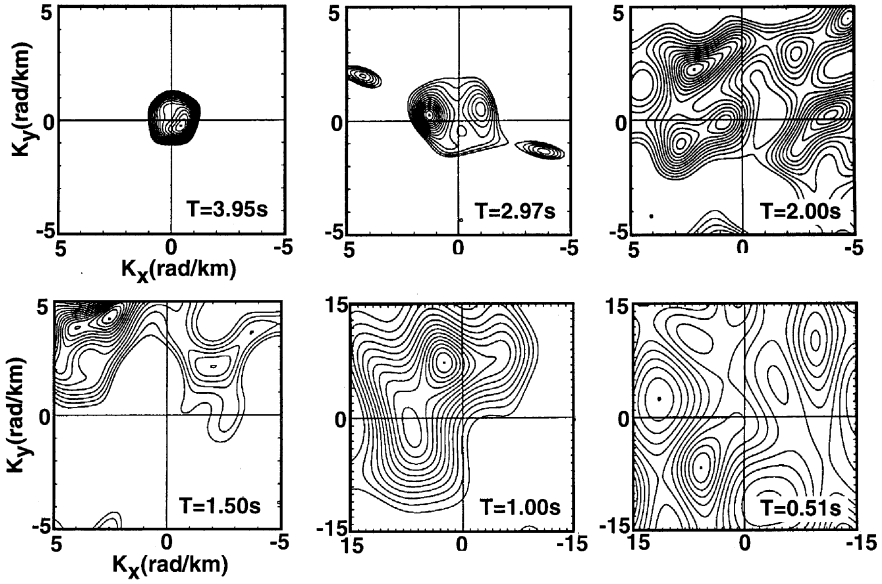

Fig. 5 Example of frequency-wavenumber spectra at NGT.

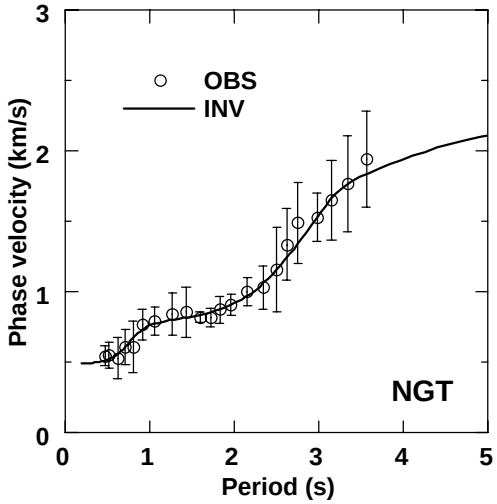

Fig. 6 Phase velocity observed at NGT.

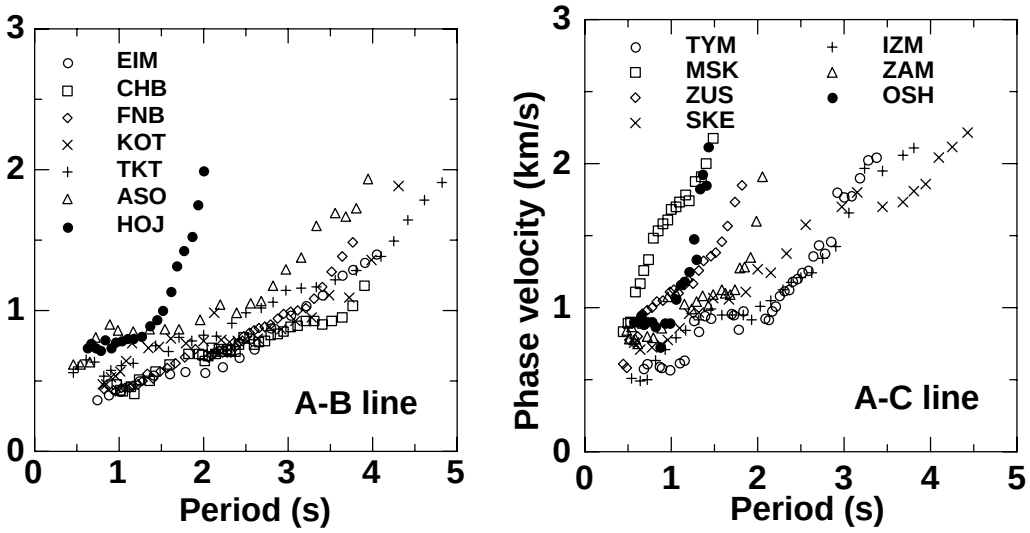

Fig. 7 Phase velocities at sites along A-B and A-C lines in Fig. 1.

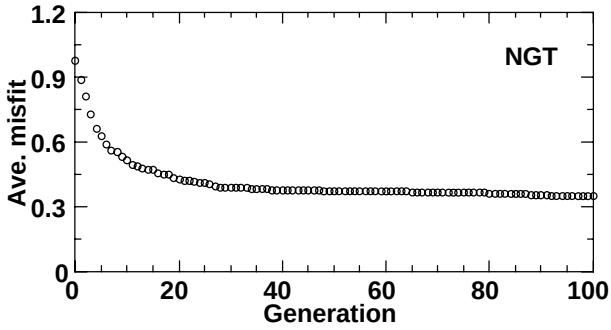

Fig. 8 Variation of misfit with increasing generation in genetic inversion of phase velocity at NGT.

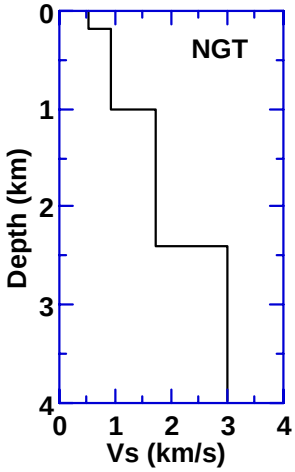

Fig. 10 S-wave models inverted from phase velocity at NGT.

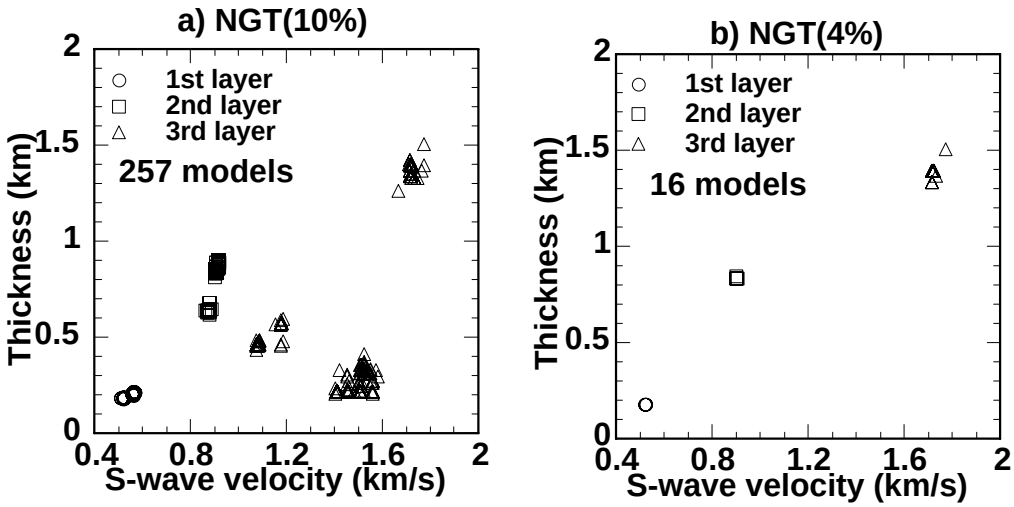

Fig. 9 Distributions of parameters of acceptable solutions in genetic inversion of phase velocity at NGT.

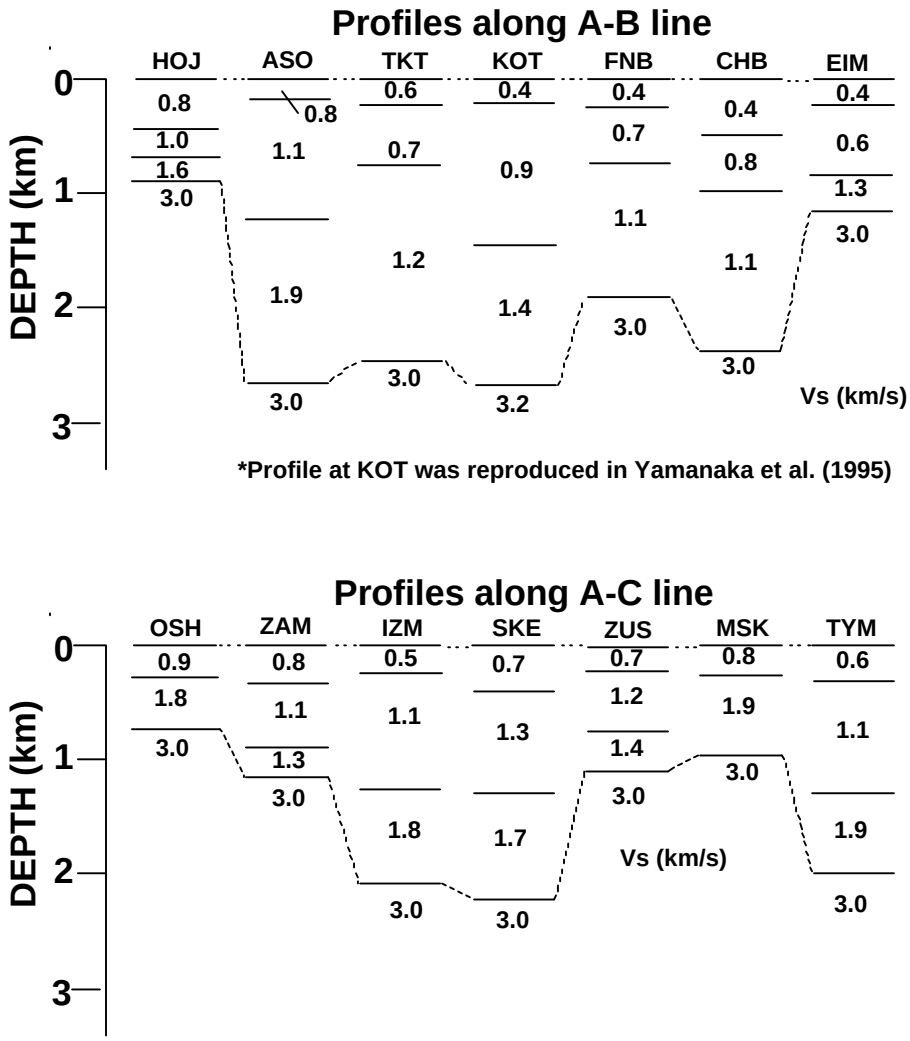

Fig. 11 S-wave proflies at sites along A-B and A-C lines in Fig. 1